NANO LETTERS

pubs.acs.org/NanoLett Letter

Real-Time Detection of Single Auger Recombination Events in a Self-Assembled Quantum Dot

Pia Lochner, Annika Kurzmann, Jens Kerski, Philipp Stegmann, Jürgen König, Andreas D. Wieck, Arne Ludwig, Axel Lorke, and Martin Geller*

Cite This: https://dx.doi.org/10.1021/acs.nanolett.9b04650 Read Online

ACCESS | Metrics & More | Article Recommendations | Supporting Information

ABSTRACT: Auger recombination is a nonradiative process, where the recombination energy of an electron–hole pair is transferred to a third charge carrier. It is a common effect in colloidal quantum dots that quenches the radiative emission with an Auger recombination time below nanoseconds. In self-assembled QDs, the Auger recombination has been observed with a much longer recombination time on the order of microseconds. Here, we use two-color laser excitation on the exciton and trion transition in resonance fluorescence on a single self-assembled quantum dot to monitor in real-time single quantum events of the Auger process. Full counting statistics on the random telegraph signal give access to the cumulants and demonstrate the tunability of the Fano factor from a Poissonian to a sub-Poissonian distribution by Auger-mediated electron emission from the dot. Therefore, the Auger process can be used to tune optically the charge carrier occupation of the dot by the incident laser intensity, independently from the electron tunneling from the reservoir by the gate voltage. Our findings are not only highly relevant for the understanding of the Auger process but also demonstrate the perspective of the Auger effect for controlling precisely the charge state in a quantum system by optical means.

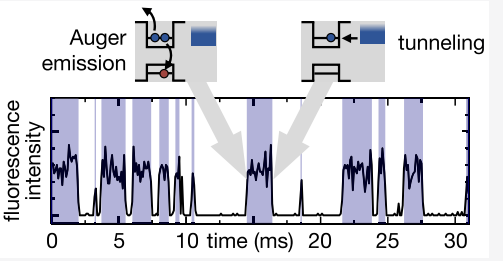

KEYWORDS: *Quantum dots, Resonance fluorescence, Auger recombination, Full counting statistics, Random telegraph signal*

The excitonic transitions in self-assembled quantum dots (QDs)[1,2] realize perfectly a two-level system in a solid-state environment. These transitions can be used to generate single-photon sources[3,4] with high photon indistinguishability,[5,6] an important prerequisite to use quantum dots as building blocks in (optical) quantum information and communication technologies.[7,8] Moreover, self-assembled QDs are still one of the best model systems to study in an "artificial atom" the carrier dynamics,[9,10] the spin- and angular-momentum properties,[11,12] and charge carrier interactions.[13] One important effect of carrier interactions is the Auger process: An electron–hole pair recombines and instead of emitting a photon, the recombination energy is transferred to a third charge carrier, which is then energetically ejected from the QD.[14−17] This is a common effect, mostly studied in colloidal QDs, where it quenches the radiative emission with recombination times on the order of picoseconds to nanoseconds.[18−20] This limits the efficiency of optical devices containing QDs like LEDs[21,22] or single-photon sources.[23−25] In self-assembled QDs, Auger recombination was speculated to be absent, and only recently, it was directly observed in optical measurements on a single self-assembled QD coupled to a charge reservoir with Auger recombination times on the order of microseconds.[26] As a single Auger process is a quantum event, it is unpredictable, and only the statistical evaluation of many such events gives access to the physical information on the recombination process.[27,28] The most in-depth evaluation—the so-called full counting statistics—becomes possible when each single quantum event in a time trace is recorded. Such real-time detection in optical experiments on a single self-assembled QD has until now only been shown for the statistical process of electron tunneling between the QD and a charge reservoir, where tunneling and spin-flip rates could be tuned by the applied electric and magnetic field.[29]

Here, Auger recombination in a single self-assembled QD is investigated by optical real-time measurements of the random telegraph signal. With the technique of two-laser excitation, we are able to detect the single quantum events of the Auger recombination. These events take place in a single QD, leaving the quantum dot empty until single-electron tunneling into the QD from the charge reservoir takes place again. This reservoir is coupled to the QD with a small tunneling rate on the order of ms^{-1}. The laser intensity, exciting the trion transition, precisely controls the electron emission by the Auger recombination and, hence, the average occupation with an electron. It also tunes the Fano factor from a Poissonian to a

Received: November 11, 2019
Revised: February 3, 2020
Published: February 5, 2020

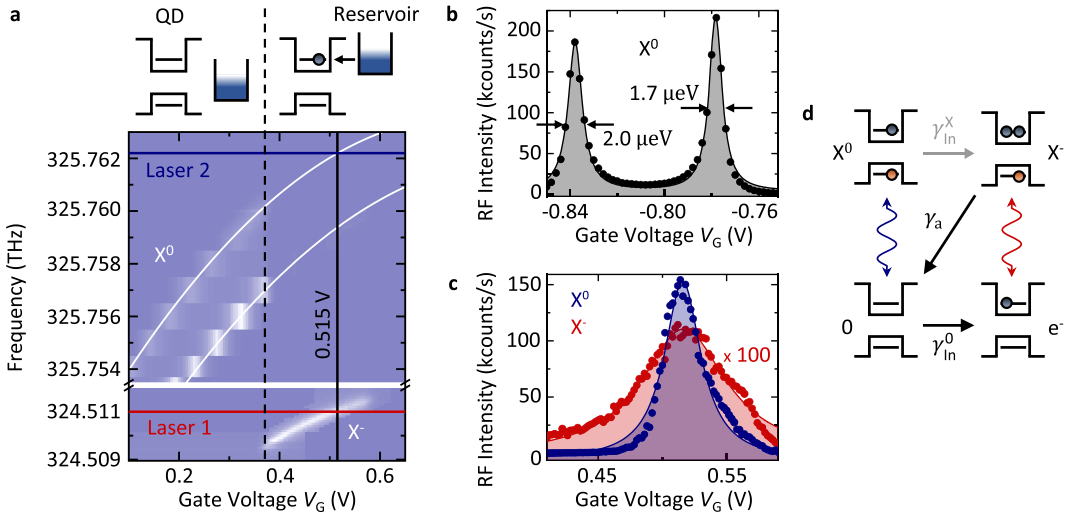

Figure 1. Resonance fluorescence (RF) of the exciton (X^0) and trion (X^-) transition. (a) Resonance fluorescence intensity as a function of excitation laser frequency and gate voltage. At gate voltages >0.375 V (vertical dashed line), the electron ground state lies below the Fermi energy of the charge reservoir. The exciton transition vanishes, and the trion transition emerges at lower frequencies. The solid lines indicate the two laser frequencies for the double-laser-excitation spectrum in Figure 1c. (b) Gate voltage scan of the exciton at a fixed excitation frequency of 325.710 THz (laser-excitation intensity of $1.6 \cdot 10^{-3}$ $\mu W/\mu m^2$). (c) Two-color laser excitation with laser 1 and laser 2 (red and blue lines in panel (a)) shows a bright exciton fluorescence X^0 at a gate voltage where, in equilibrium, an electron would occupy the QD and quenches the X^0 transition. X^- signal is scaled up by a factor of 100. Simultaneous excitation of the trion transition X^- empties the dot by Auger recombination, and the exciton transition can be excited with the second laser until an electron tunnels into the dot again. (d) Schematic representation of the different dot states (counterclockwise, from bottom left): empty dot; single-electron occupation; trion state; exciton state. Wavy double arrows indicate optical transitions, straight arrows symbolize (top to bottom, including the respective rates γ) electron tunneling into the trion state, Auger recombination, and tunneling into the empty dot.

sub-Poissonian distribution, which we observe in analyzing the random telegraph signal by methods of full counting statistics.

The investigated sample was grown by molecular beam epitaxy (MBE) with a single layer of self-assembled In(Ga)As QDs embedded in a p−i−n diode (see Supporting Information for details). A highly n-doped GaAs layer acts as a charge reservoir, which is coupled to the QDs via a tunneling barrier, while a highly p-doped GaAs layer defines an epitaxial gate.[30] An applied gate voltage V_G shifts energetically the QD states with respect to the Fermi energy in the electron reservoir and controls the charge state of the dots by electron tunneling through the tunneling barrier. The sample is integrated into a confocal microscope setup within a bath cryostat at 4.2 K for resonance fluorescence (RF) measurements (see Methods).

Figure 1 shows the RF of the neutral exciton (X^0) and the negatively charged exciton, called a trion (X^-). A RF measurement as a function of gate voltage in Figure 1b shows the fine-structure split exciton[31] with an average line width of about 1.8 μeV at low excitation intensity ($1.6 \cdot 10^{-3}$ $\mu W/\mu m^2$). Note that this is an equilibrium spectrum of the neutral exciton, which cannot be taken in the frequency range of "Laser 2". At gate voltages ≥0.375 V, an additional electron occupies the dot, and the X^0 can only be excited when the electron is removed and the dot is in a nonequilibrium configuration.

The quantum-confined Stark effect shifts the exciton resonance X^0 for higher gate voltages to higher frequencies up to 325.760 THz, as seen in Figure 1a. This quadratic Stark shift of the two exciton transitions[32] is indicated by two white lines. At a voltage of about 0.375 V (dashed vertical line in Figure 1a), the electron ground state in the dot is in resonance with the Fermi energy in the charge reservoir. An electron tunnels into the QD and the exciton transition vanishes while the trion transition can be excited at lower frequencies from 324.5095 to 324.5115 THz.

The spectrum of the exciton (blue dots) and the trion transition (red dots) under two-laser excitation is shown in Figure 1c. The trion transition is measured at a laser frequency of 324.511 THz (corresponding to the red line, "Laser 1" in Figure 1a) and a laser-excitation intensity of $8 \cdot 10^{-6}$ $\mu W/\mu m^2$ at a gate voltage of 0.515 V. The exciton spectrum in Figure 1c was obtained simultaneously by a second laser 2 on the exciton transition (blue line in Figure 1a at 325.7622 THz) with a laser-excitation intensity of $1.6 \cdot 10^{-3}$ $\mu W/\mu m^2$, as the Auger recombination with rate γ_a leads to an empty QD until an electron tunnels into the dot from the reservoir with rate γ_{In}. This rate comprises the tunneling into the empty dot and the tunneling into the dot charged with an exciton, which is much less probable (see Figure 1d for a schematic representation). This has been explained previously in Kurzmann et al.[26] with the important conclusion that the intensity ratio between trion/exciton intensity in equilibrium measurements is given by the ratio between Auger/tunneling rate γ_a/γ_{In}.

The weak coupling between the reservoir and the quantum dot in the present sample leads to very long electron tunneling times compared to common p−i−n diode designs. Therefore, the interplay between electron tunneling and optical-driven Auger recombination can be studied in more detail by a real-time random telegraph signal of the resonance fluorescence. In these measurements, the time stamp of every detected RF photon is recorded, see Figure 2, enabling the evaluation by full counting statistics. As the intensity of the trion is very weak, the random telegraph signal has been investigated in a two-color excitation scheme. The bright exciton transition with count rates exceeding 10 Mcounts/s (see Supporting Information) is used as an optical detector for the telegraph signal of the Auger recombination. In this two-color laser-

https://dx.doi.org/10.1021/acs.nanolett.9b04650
Nano Lett. XXXX, XXX, XXX−XXX

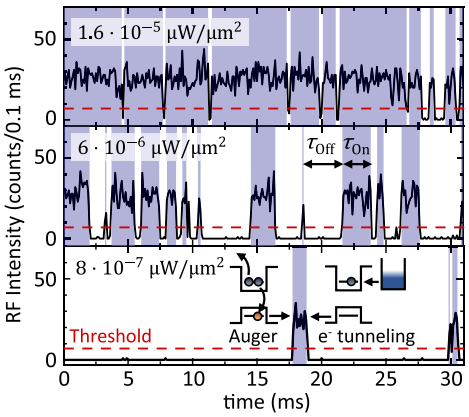

Figure 2. Time-resolved RF random telegraph signal. At a gate voltage of 0.515 V, the trion and exciton are excited simultaneously (like in Figure 1c). The intensity of the exciton excitation laser 2 is held constant at $1.6 \cdot 10^{-3}$ $\mu W/\mu m^2$, which is far below the saturation of the RF signal (see Supporting Information). The intensity of the trion excitation laser 1 is varied (from top to bottom: $1.6 \cdot 10^{-5}$, $6 \cdot 10^{-6}$, and $8 \cdot 10^{-7}$ $\mu W/\mu m^2$). Every time an Auger recombination takes place, the dot is emptied, and exciton RF signal turns on. After a time τ_{On}, an electron tunnels into the QD, and the exciton RF signal quenches. All intensities smaller than the threshold (red line at 7 counts/0.1 ms) are counted as "exciton off" (white areas); all intensities above the threshold are counted as "exciton on" (blue areas).

excitation scheme, the "exciton off" signal corresponds to the "trion on" signal and vice versa.[26] Hence, the trion statistics can directly be determined from the "inverse" exciton signal. The intensity of the exciton excitation laser 2 is held constant at $1.6 \cdot 10^{-3}$ $\mu W/\mu m^2$. This intensity is far below the saturation of the RF signal of the exciton (see Supporting Information) and avoids the photon-induced electron capture at high excitation intensities.[33] However, this laser intensity yields count rates above 200 kcounts/s (see Figure 1b), sufficiently high for recording single quantum events in a real-time measurement.[29] While the intensity of the exciton detection laser 2 is kept constant, the laser intensity of the trion excitation laser 1 is increased from $1.6 \cdot 10^{-7}$ up to $1.6 \cdot 10^{-5}$ $\mu W/\mu m^2$.

For every trion laser intensity, the time-resolved RF signal is recorded for 15 min using a fast (350 ps) avalanche photodiode and a bin time of 100 μs. Figure 2 shows parts of three different time traces at three different trion laser 1 intensities. As the exciton laser 2 intensity always exceeds the trion laser 1 intensity by at least nearly 2 orders of magnitude, the small amount of RF counts from the trion can be neglected. As a consequence, the detected RF signal of the exciton is directly related to the Auger recombination: An Auger recombination empties the dot, and the exciton transition detects an empty dot (no trion transition possible) with a count rate of about 25 counts per bin time (100 μs). After a time τ_{On}, an electron tunnels into the QD (see Figure 2), and the exciton RF signal quenches until, after a time τ_{Off}, another Auger recombination happens.

Increasing the trion laser intensity from $8 \cdot 10^{-7}$ up to $1.6 \cdot 10^{-5}$ $\mu W/\mu m^2$ in Figure 2 increases the probability of an Auger emission with rate $\gamma_E = n\gamma_a$, as the probability for occupation n of the dot with a trion increases with increasing laser 1 intensity. Therefore, the exciton transition is observed most frequently for the highest trion laser intensity. This can be observed in Figure 2, where the optical random telegraph signal is compared for three different trion excitation intensities. A threshold between exciton "on" and "off" is set for the following statistical evaluation.[34,35] All exciton RF intensities smaller than this threshold (dashed red line at 7 counts/0.1 ms in Figure 2) are counted as "exciton off" (white areas), and all intensities above the threshold are counted as "exciton on" (blue areas).

From these time-resolved RF data sets, the Auger and tunneling rates can be determined by analyzing the probability distributions of the "off" times τ_{Off} and the "on" times τ_{On} for every 15 min long data set.[34] A representative distribution at a trion laser intensity of $8 \cdot 10^{-7}$ $\mu W/\mu m^2$ can be seen in Figure 3a. An exponential fit to the "on" times (blue line in Figure 3a) yields the tunneling rate γ_{In} into the QD, while an exponential fit to the "off" times (red line in Figure 3a) yields the emission rate $\gamma_E = n\gamma_a$ for this specific trion laser 1 intensity. In the example in Figure 3a, we find $\gamma_{In} = 0.80$ ms^{-1} and $\gamma_E = 0.074$ ms^{-1}. As discussed above, the probability for emitting an electron by an Auger recombination process increases with the probability n, that the dot is occupied with a trion.

The trion occupation probability n as a function of the laser 1 excitation power was determined from a pulsed measurement of the trion RF intensity (see Figure S4 in the Supporting Information). In the relevant range of laser powers ($\leq 1.6 \cdot 10^{-5}$ $\mu W/\mu m^2$), the dependence is linear. Since Auger recombination can only take place when a trion is present in

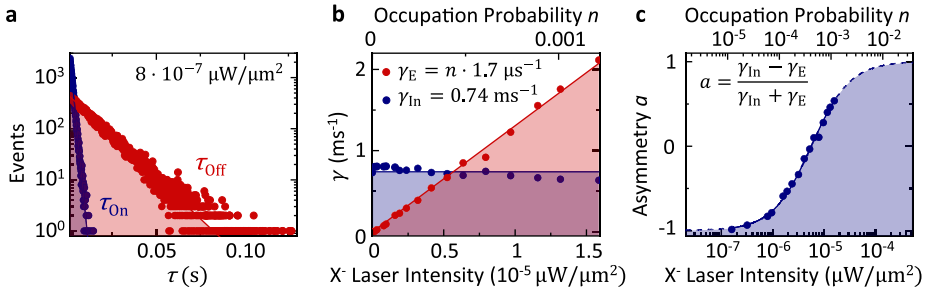

Figure 3. Auger and tunneling rates from the time-resolved RF random telegraph signal. Panel (a) shows the probability distribution of the "off" (red dots) and "on" times (blue dots) from the measurement at $8 \cdot 10^{-7}$ $\mu W/\mu m^2$ trion laser-excitation intensity (laser 1). Fitting these data yields the emission rate $\gamma_E = n\gamma_a$ and the tunneling rate of an electron into the dot γ_{In}. In panel (b), the emission and tunneling rates are plotted as a function of the trion laser intensity (red and blue dots, respectively). The tunneling rate remains constant at a mean value of 0.74 ms^{-1}, the emission rate increases linearly with the laser intensity and, accordingly, with the occupation probability n (top axis). (c) Asymmetry a, calculated from the emission and tunneling rates as shown in the inset, as a function of the trion laser intensity.

https://dx.doi.org/10.1021/acs.nanolett.9b04650
Nano Lett. XXXX, XXX, XXX−XXX

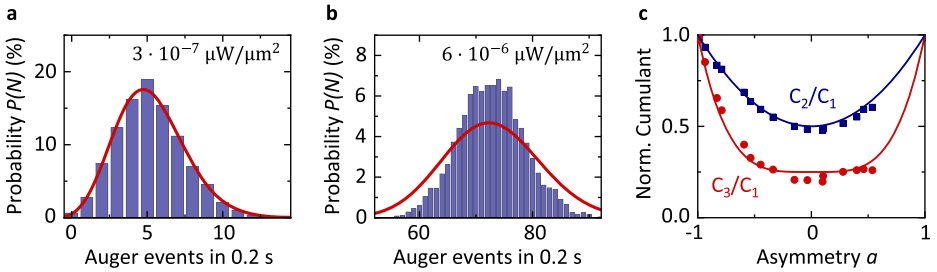

Figure 4. Probability distribution and cumulants of the time-resolved RF random telegraph signal. Panels (a) and (b) show the probability $P(N)$ for a number N of Auger events in a bin time of 200 ms (blue bars) and the Poissonian distribution related to the mean value of the probability $P(N)$ (red curve). At a trion excitation intensity (laser 1) of $3 \cdot 10^{-7}$ μW/μm^2 (panel (a)), which corresponds to an asymmetry close to −1, the probability $P(N)$ is close to a Poissonian distribution. At a trion excitation intensity of $6 \cdot 10^{-6}$ μW/μm^2 (panel (b)), which corresponds to an asymmetry close to 0, the probability $P(N)$ is sub-Poissonian. Panel (c) shows the second (blue) and third (red) normalized cumulants as a function of the asymmetry. Symbols are measured values, and lines are calculated curves for a two-state system.[35]

the dot, the electron emission rate is expected to be proportional to n. Figure 3b shows the resulting overall linear dependence of the electron emission rate γ_E on the trion (X^-) intensity. Tunable emission rates between approximately 0 and $\gamma_E \approx 2$ ms^{-1} could be achieved. The proportionality factor between the occupation probability n and the emission rate $\gamma_E = n\,\gamma_A$ is the intrinsic Auger rate γ_A, i.e., the rate with which a given trion will recombine by the Auger effect. We find $\gamma_A = 1.7$ μs^{-1} (solid red line in Figure 3b) in good agreement with the value obtained independently for a QD with a slightly different size.[26] The tunneling rate γ_{In} is unaffected by the X^- laser intensity and remains approximately constant at around 0.74 ms^{-1} (blue data points in Figure 3b). This has two reasons: (1) The (constant) X^0 laser intensity of $1.6 \cdot 10^{-3}$ μW/μm^2 is orders of magnitude higher than the X^- laser intensity so that changing the latter will have a negligible effect on the tunneling dynamics. (2) Before the tunneling event, the (empty) dot will be transparent for the X^- laser wavelength, as the trion excitation requires that an electron is already present in the dot. We are thus able to not only adjust the tunneling rate by appropriately setting the gate voltage. We can also, independently, use the Auger recombination to optically tune the electron emission rate. An independent tuning of electron emission and capture rate is usually not possible for a QD that is tunnel-coupled to one charge reservoir. Changing the coupling strength or Fermi energy by a gate voltage always changes both rates for tunneling into and out of the dot simultaneously.

Using the standard methods of full counting statistics[34,36] in the following, first of all the asymmetry $a = \frac{\gamma_{In} - \gamma_E}{\gamma_{In} + \gamma_E}$ between the tunneling γ_{In} and emission rate γ_E has been evaluated. The asymmetry in Figure 3c can be tuned by the trion excitation laser intensity from −1 up to 0.55 at a maximum laser intensity of $1.6 \cdot 10^{-5}$ μW/μm^2. It is important to mention here that at high trion laser intensities above $1.6 \cdot 10^{-5}$ μW/μm^2, the electron emission by Auger recombination after a tunneling event from the reservoir happens much faster than the bin time of 0.1 ms. Therefore, the RF intensity within the bin time is not falling below the threshold, and these events are not detected, i.e. the maximum bandwidth of 10 kHz (given by the bin time) of the optical detection scheme distorts the statistical analysis at trion laser intensities above $1.6 \cdot 10^{-5}$ μW/μm^2. Below this laser intensity, every single Auger recombination event is detected in the real-time telegraph signal.

Finally, full counting statistics[34,37,38] is performed on the telegraph signal: Every 15 min long telegraph signal is divided into sections with length t_0. The number N of Auger events within the time interval t_0 is counted. Figure 4a,b shows two examples for the corresponding probability distributions $P(N)$ in the limit of large t_0 (0.2 s). At an asymmetry close to −1 (a trion laser intensity of $3 \cdot 10^{-7}$ W/m^2, Figure 4a), the probability is close to a Poissonian distribution. At an asymmetry of about 0 (laser intensity of $6 \cdot 10^{-6}$ μW/μm^2, Figure 4b), the probability distribution is sub-Poissonian, indicating a correlation between Auger recombination and electron tunneling: The Auger recombination can only take place after an electron has tunneled from the reservoir into the dot. Vice versa, the electron can only tunnel after the Auger recombination has emptied the QD. From the probability distributions, the cumulants $C_m(t_0) = \partial_z^m \ln \mathcal{M}(z, t_0)|_{z=0}$ can be derived with the generating function $\mathcal{M}(z, t_0) = \sum_N e^{zN} P(N)$.[34] The first cumulant C_1 corresponds to the mean value, the second cumulant C_2 is the variance, and the third cumulant describes the skewedness of the distribution. The second and third normalized cumulants in the limit of large t_0 (20 and 5 ms, respectively) can be seen as data points in Figure 4c. For a two-state system in the long-time limit, theory predicts $C_2/C_1 = (1 + a^2)/2$ (also called the "Fano factor") and $C_3/C_1 = (1 + 3a^4)/4$,[35] shown as lines in Figure 4c. The data for the second and third normalized cumulants coincide well with the calculated curves. We can conclude from the statistical analysis that the QD behaves like a two-state system, where one state is the QD charged with one electron (or a trion after optical excitation) and the other state is the empty dot (or charged with an exciton). The QD charged with one electron cannot be distinguished from the dot containing a trion (same for empty dot and exciton), as the optical transition times on the order of nanoseconds are orders of magnitude faster than the tunneling and emission time by the Auger recombination.[39] The statistical analysis demonstrates the influence of the Auger recombination on the cumulants, especially on the Fano factor, which can be tuned from $F = 1$ to $F = 0.5$ by increasing the incident laser intensity on the trion transition.

In summary, we performed real-time RF random telegraph measurements and studied full counting statistics of the Auger effect in a single self-assembled QD. With this technique, we were able to measure single Auger recombination events as quantum jumps from a charged to an uncharged QD, followed by single-electron tunneling. The full counting statistics give access to the normalized cumulants and demonstrate the tunability of the Fano factor from Possonian to sub-Poissonian distribution by the incident laser intensity on the trion

https://dx.doi.org/10.1021/acs.nanolett.9b04650
Nano Lett. XXXX, XXX, XXX−XXX

transition. Comparison with theoretical prediction shows that the empty and charged QD with the Auger recombination and tunneling follows a dynamical two-state system. For future quantum-state preparation, the Auger process can be used to control the charge state in a quantum system by optical means.

METHODS

As the same measurement technique is used, this methods section follows the Supporting Information of Kurzmann et al.[29]

Optical Measurements. Resonant optical excitation and collection of the fluorescence light is used to detect the optical response of the single self-assembled QD, where the resonance condition is achieved by applying a specific gate voltage between the gate electrode and the Ohmic back contact. The QD sample is mounted on a piezo-controlled stage under an objective lens with a numerical aperture of NA = 0.65, giving a focal spot size of about 1 μm diameter. All experiments are carried out in a liquid He confocal dark-field microscope at 4.2 K with a tunable diode laser for excitation and an avalanche photodiode (APD) for fluorescence detection. The resonant laser excitation and fluorescence detection are aligned along the same path with a microscope head that contains a 90:10 beam splitter and two polarizers. Cross-polarization enables a suppression of the spurious laser scattering into the detection path by a factor of more than 10^7. The counts of the APD (dead time of 21.5 ns) were binned by a QuTau time-to-digital converter with a temporal resolution of 81 ps.

ASSOCIATED CONTENT

Supporting Information

The Supporting Information is available free of charge at https://pubs.acs.org/doi/10.1021/acs.nanolett.9b04650.

Sample and device fabrication and excitation laser intensity-dependent resonance fluorescence (PDF)

AUTHOR INFORMATION

Corresponding Author

Martin Geller − *Faculty of Physics and CENIDE, University of Duisburg-Essen, 47057 Duisburg, Germany;* orcid.org/0000-0003-3796-1908; Email: martin.geller@uni-due.de

Authors

Pia Lochner − *Faculty of Physics and CENIDE, University of Duisburg-Essen, 47057 Duisburg, Germany*

Annika Kurzmann − *Faculty of Physics and CENIDE, University of Duisburg-Essen, 47057 Duisburg, Germany; Solid State Physics Laboratory, ETH Zurich, 8093 Zurich, Switzerland;* orcid.org/0000-0001-5947-0400

Jens Kerski − *Faculty of Physics and CENIDE, University of Duisburg-Essen, 47057 Duisburg, Germany*

Philipp Stegmann − *Faculty of Physics and CENIDE, University of Duisburg-Essen, 47057 Duisburg, Germany*

Jürgen König − *Faculty of Physics and CENIDE, University of Duisburg-Essen, 47057 Duisburg, Germany*

Andreas D. Wieck − *Lehrstuhl für Angewandte Festkörperphysik, Ruhr-Universität Bochum, 44780 Bochum, Germany*

Arne Ludwig − *Lehrstuhl für Angewandte Festkörperphysik, Ruhr-Universität Bochum, 44780 Bochum, Germany*

Axel Lorke − *Faculty of Physics and CENIDE, University of Duisburg-Essen, 47057 Duisburg, Germany;* orcid.org/0000-0002-0405-7720

Complete contact information is available at: https://pubs.acs.org/10.1021/acs.nanolett.9b04650

Notes

The authors declare no competing financial interest.

ACKNOWLEDGMENTS

This work was supported by the German Research Foundation (DFG) within the Collaborative Research Centre (SFB) 1242, Project No. 278162697 (TP A01 and A02), and the individual research grant No. GE2141/5-1. A. Lu acknowledges gratefully support of the DFG by project LU2051/1-1 and together with A.D.W. acknowledges support by DFG-TRR160, BMBF - Q.Link.X 16KIS0867, and the DFH/UFA CDFA-05-06.

REFERENCES

(1) Bimberg, D.; Grundmann, M.; Ledentsov, N. N. *Quantum Dot Heterostructures*; John Wiley & Sons, 1999.

(2) Petroff, P. M.; Lorke, A.; Imamoglu, A. Epitaxially Self-Assembled Quantum Dots. *Phys. Today* **2001**, *54*, 46−52.

(3) Michler, P. A Quantum Dot Single-Photon Turnstile Device. *Science* **2000**, *290*, 2282−2285.

(4) Yuan, Z. Electrically Driven Single-Photon Source. *Science* **2002**, *295*, 102−105.

(5) Santori, C.; Fattal, D.; Vučković, J.; Solomon, G. S.; Yamamoto, Y. Indistinguishable photons from a single-photon device. *Nature* **2002**, *419*, 594−597.

(6) Matthiesen, C.; Geller, M.; Schulte, C. H.; Le Gall, C.; Hansom, J.; Li, Z.; Hugues, M.; Clarke, E.; Atatüre, M. Phase-locked indistinguishable photons with synthesized waveforms from a solid-state source. *Nat. Commun.* **2013**, *4*, 1600.

(7) Kimble, H. J. The quantum internet. *Nature* **2008**, *453*, 1023−1030.

(8) Ladd, T. D.; Jelezko, F.; Laflamme, R.; Nakamura, Y.; Monroe, C.; O'Brien, J. L. Quantum computers. *Nature* **2010**, *464*, 45−53.

(9) Kurzmann, A.; Merkel, B.; Labud, P.; Ludwig, A.; Wieck, A.; Lorke, A.; Geller, M. Optical blocking of electron tunneling into a single self-assembled quantum dot. *Phys. Rev. Lett.* **2016**, *117*, No. 017401.

(10) Geller, M. Nonequilibrium carrier dynamics in self-assembled quantum dots. *Appl. Phys. Rev.* **2019**, *6*, No. 031306.

(11) Bayer, M.; Stern, O.; Hawrylak, P.; Fafard, S.; Forchel, A. Hidden symmetries in the energy levels of excitonic artificial atoms'. *Nature* **2000**, *405*, 923−926.

(12) Vamivakas, A. N.; Zhao, Y.; Lu, C.-Y.; Atatüre, M. Spin-resolved quantum-dot resonance fluorescence. *Nat. Phys.* **2009**, *5*, 198−202.

(13) Labud, P.; Ludwig, A.; Wieck, A.; Bester, G.; Reuter, D. Direct Quantitative Electrical Measurement of Many-Body Interactions in Exciton Complexes in In As Quantum Dots. *Phys. Rev. Lett.* **2014**, *112*, No. 046803.

(14) Kharchenko, V.; Rosen, M. Auger relaxation processes in semiconductor nanocrystals and quantum wells. *J. Lumin.* **1996**, *70*, 158−169.

(15) Efros, A. L.; Rosen, M. Random Telegraph Signal in the Photoluminescence Intensity of a Single Quantum Dot. *Phys. Rev. Lett.* **1997**, *78*, 1110−1113.

(16) Fisher, B.; Caruge, J.-M.; Chan, Y.-T.; Halpert, J.; Bawendi, M. G. Multiexciton fluorescence from semiconductor nanocrystals. *Chem. Phys.* **2005**, *318*, 71−81.

(17) Jha, P. P.; Guyot-Sionnest, P. Trion Decay in Colloidal Quantum Dots. *ACS Nano* **2009**, *3*, 1011−1015.

(18) Vaxenburg, R.; Rodina, A.; Shabaev, A.; Lifshitz, E.; Efros, A. L. Nonradiative Auger Recombination in Semiconductor Nanocrystals. *Nano Lett.* **2015**, *15*, 2092−2098.
(19) Klimov, V. I. Quantization of Multiparticle Auger Rates in Semiconductor Quantum Dots. *Science* **2000**, *287*, 1011−1013.
(20) Park, Y.-S.; Bae, W. K.; Pietryga, J. M.; Klimov, V. I. Auger Recombination of Biexcitons and Negative and Positive Trions in Individual Quantum Dots. *ACS Nano* **2014**, *8*, 7288−7296.
(21) Caruge, J. M.; Halpert, J. E.; Wood, V.; Bulović, V.; Bawendi, M. G. Colloidal quantum-dot light-emitting diodes with metal-oxide charge transport layers. *Nat. Photonics* **2008**, *2*, 247−250.
(22) Cho, K.-S.; Lee, E. K.; Joo, W.-J.; Jang, E.; Kim, T.-H.; Lee, S. J.; Kwon, S.-J.; Han, J. Y.; Kim, B.-K.; Choi, B. L.; Kim, J. M. High-performance crosslinked colloidal quantum-dot light-emitting diodes. *Nat. Photonics* **2009**, *3*, 341−345.
(23) Brokmann, X.; Messin, G.; Desbiolles, P.; Giacobino, E.; Dahan, M.; Hermier, J. P. Colloidal CdSe/ZnS quantum dots as single-photon sources. *New J. Phys.* **2004**, *6*, 99.
(24) Michler, P.; Imamoğlu, A.; Mason, M. D.; Carson, P. J.; Strouse, G. F.; Buratto, S. K. Quantum correlation among photons from a single quantum dot at room temperature. *Nature* **2000**, *406*, 968−970.
(25) Lounis, B.; Bechtel, H.; Gerion, D.; Alivisatos, P.; Moerner, W. Photon antibunching in single CdSe/ZnS quantum dot fluorescence. *Chem. Phys. Lett.* **2000**, *329*, 399−404.
(26) Kurzmann, A.; Ludwig, A.; Wieck, A. D.; Lorke, A.; Geller, M. Auger Recombination in Self-Assembled Quantum Dots: Quenching and Broadening of the Charged Exciton Transition. *Nano Lett.* **2016**, *16*, 3367−3372.
(27) Levitov, L. S.; Lee, H.; Lesovik, G. B. Electron counting statistics and coherent states of electric current. *J. Math. Phys.* **1996**, *37*, 4845−4866.
(28) Blanter, Y.; Büttiker, M. Shot noise in mesoscopic conductors. *Phys. Rep.* **2000**, *336*, 1−166.
(29) Kurzmann, A.; Stegmann, P.; Kerski, J.; Schott, R.; Ludwig, A.; Wieck, A.; König, J.; Lorke, A.; Geller, M. Optical Detection of Single-Electron Tunneling into a Semiconductor Quantum Dot. *Phys. Rev. Lett.* **2019**, *122*, 247403.
(30) Ludwig, A.; Prechtel, J. H.; Kuhlmann, A. V.; Houel, J.; Valentin, S. R.; Warburton, R. J.; Wieck, A. D. Ultra-low charge and spin noise in self-assembled quantum dots. *J. Cryst. Growth* **2017**, *477*, 193−196.
(31) Högele, A.; Seidl, S.; Kroner, M.; Karrai, K.; Warburton, R. J.; Gerardot, B. D.; Petroff, P. M. Voltage-Controlled Optics of a Quantum Dot. *Phys. Rev. Lett.* **2004**, *93*, 217401.
(32) Li, S.-S.; Xia, J.-B. Quantum-confirned Stark effects of InAs/GaAs self-assembled quantum dot. *J. Appl. Phys.* **2000**, *88*, 7171−7174.
(33) Kurzmann, A.; Ludwig, A.; Wieck, A. D.; Lorke, A.; Geller, M. Photoelectron generation and capture in the resonance fluorescence of a quantum dot. *Appl. Phys. Lett.* **2016**, *108*, 263108.
(34) Gustavsson, S.; Leturcq, R.; Studer, M.; Shorubalko, I.; Ihn, T.; Ensslin, K.; Driscoll, D.; Gossard, A. Electron counting in quantum dots. *Surf. Sci. Rep.* **2009**, *64*, 191−232.
(35) Gustavsson, S.; Leturcq, R.; Simovič, B.; Schleser, R.; Ihn, T.; Studerus, P.; Ensslin, K.; Driscoll, D. C.; Gossard, A. C. Counting Statistics of Single Electron Transport in a Quantum Dot. *Phys. Rev. Lett.* **2006**, *96*, No. 076605.
(36) Flindt, C.; Fricke, C.; Hohls, F.; Novotny, T.; Netocny, K.; Brandes, T.; Haug, R. J. Universal oscillations in counting statistics. *Proc. Natl. Acad. Sci. U. S. A.* **2009**, *106*, 10116−10119.
(37) Fricke, C.; Hohls, F.; Wegscheider, W.; Haug, R. J. Bimodal counting statistics in single-electron tunneling through a quantum dot. *Phys. Rev. B: Condens. Matter Mater. Phys.* **2007**, *76*, 155307.
(38) Gorman, S.; He, Y.; House, M.; Keizer, J.; Keith, D.; Fricke, L.; Hile, S.; Broome, M.; Simmons, M. Tunneling Statistics for Analysis of Spin-Readout Fidelity. *Phys. Rev. Appl.* **2017**, *8*, No. 034019.
(39) Zrenner, A.; Beham, E.; Stufler, S.; Findeis, F.; Bichler, M.; Abstreiter, G. Coherent properties of a two-level system based on a quantum-dot photodiode. *Nature* **2002**, *418*, 612−614.

https://dx.doi.org/10.1021/acs.nanolett.9b04650
Nano Lett. XXXX, XXX, XXX−XXX